

Surface States Transport in Topological Insulator $\text{Bi}_{0.83}\text{Sb}_{0.17}$ Nanowires

L. A. Konopko^{1,2} · A. A. Nikolaeva^{1,2} ·
T. E. Huber³ · J.-P. Ansermet⁴

Received: 25 June 2015 / Accepted: 12 January 2016 / Published online: 27 January 2016
© Springer Science+Business Media New York 2016

Abstract We investigate the transport properties of topological insulator (TI) $\text{Bi}_{0.83}\text{Sb}_{0.17}$ nanowires. Single-crystal nanowire samples with diameters ranging from 75 nm to 1.1 μm are prepared using high frequency liquid phase casting in a glass capillary; cylindrical single crystals with (10 $\bar{1}$ 1) orientation along the wire axis are produced. $\text{Bi}_{0.83}\text{Sb}_{0.17}$ is a narrow-gap semiconductor with an energy gap at the L point of the Brillouin zone, $\Delta E = 21$ meV. The resistance of the samples increases with decreasing temperature, but a decrease in resistance is observed at low temperatures. This effect is a clear manifestation of TI properties (i.e., the presence of a highly conducting zone on the TI surface). When the diameter of the nanowire decreases, the energy gap ΔE grows as $1/d$ (for diameter $d = 1.1\mu\text{m}$ and $d = 75$ nm $\Delta E = 21$ and 45 meV, respectively), which proves the presence of the quantum size effect in these samples. We investigate the magnetoresistance of $\text{Bi}_{0.83}\text{Sb}_{0.17}$ nanowires at various magnetic field orientations. Shubnikov-de Haas oscillations are observed in $\text{Bi}_{0.83}\text{Sb}_{0.17}$ nanowires at $T = 1.5$ K, demonstrating the existence of high mobility ($\mu_S = 26,700 - -47,000$ cm²V⁻¹s⁻¹) two-dimensional (2D) carriers in the surface areas of the nanowires, which are nearly perpendicular to the C_3 axis. From the linear dependence of the nanowire conductance on nanowire diameter at $T = 4.2$ K, the square resistance R_{sq} of the surface states of the nanowires is obtained ($R_{\text{sq}} = 70$ Ohm).

✉ L. A. Konopko
l.konopko@nano.asm.md

¹ Ghitu Institute of Electronic Engineering and Nanotechnologies, 2028 Chisinau, Moldova
² International Laboratory of High Magnetic Fields and Low Temperatures, 53-421 Wroclaw, Poland
³ Department of Chemistry, Howard University, Washington, DC 20059, USA
⁴ LPMN, École Polytechnique Fédérale de Lausanne EPFL, 1015 Lausanne, Switzerland

Keywords Surface states · Topological insulator · Bi-Sb · Single-crystal nanowires · Quantum oscillations

1 Introduction

A topological insulator (TI), which is topologically distinct from an ordinary insulator, is a material with a bulk electronic excitation gap generated by the spin-orbit interaction. This distinction, characterized by a Z_2 topological invariant, necessitates the existence of gapless electronic states on the sample boundary. In two dimensions (2D), the TI is a quantum spin Hall insulator. A strong TI is expected to have surface states whose Fermi surfaces enclose an odd number of Dirac points. This defines a topological metal surface phase that is predicted to have novel electronic properties. The first TI to be discovered was the alloy $\text{Bi}_{1-x}\text{Sb}_x$, the unusual surface bands of which were mapped in an angle-resolved photoemission spectroscopy (ARPES) experiment [1,2]. The semiconducting alloy $\text{Bi}_{1-x}\text{Sb}_x$ is a strong TI owing to the inversion symmetry of bulk crystalline Bi and Sb.

In recent decades, considerable attention has been paid to bismuth-antimony alloys ($\text{Bi}_{1-x}\text{Sb}_x$) of various compositions. This class of materials is considered to be one of the best candidates for thermoelectric application in the cryogenic temperature range. Bismuth is a semimetal with strong spin-orbit interactions, which has an indirect negative gap between the valence band at the T point of the bulk Brillouin zone and the conduction band at the L points [3,4]. Substituting bismuth with antimony changes the critical energies of the band structure (see Fig. 1a). At an Sb concentration of $x = 0.04$, the gap ΔE between L_a and L_s closes, and the massless, three-dimensional (3D) Dirac point is created. At concentrations greater than $x = 0.09$, the system develops into a direct-gap insulator, the low-energy physics of which is dominated by the spin-orbit coupled Dirac particles at L [5]. Here we study nanowires with $x = 0.17$, that in the bulk, are semiconductors with an L -point gap of 21 meV.

The unusual metallic surfaces of these TIs may result in the development of new spintronic or magnetoelectric devices. Furthermore, in combination with superconductors, TIs could lead to a new architecture for topological quantum bits.

In the present paper, we report measurements of the temperature dependence of resistance as well as those of magnetic field dependence of the magnetoresistance of TI $\text{Bi}_{0.83}\text{Sb}_{0.17}$ nanowires in glass coating.

2 Experimental

Individual $\text{Bi}_{0.83}\text{Sb}_{0.17}$ nanowires were fabricated using the Ulitovsky technique (see schematic diagram in inset of Fig. 1b). This technique involves a high-frequency induction coil melting of a $\text{Bi}_{0.83}\text{Sb}_{0.17}$ boule within a borosilicate glass (Pyrex) capsule in an argon atmosphere, simultaneously softening the glass. Glass capillaries, each containing a $\text{Bi}_{0.83}\text{Sb}_{0.17}$ filament [6], were produced by drawing material from the glass. Nanowire samples with diameters ranging from 75 nm to 1.1 μm were prepared. The nanowires are single crystals with $(10\bar{1}1)$ orientation along the wire axis. In this orientation, the wire axis makes an angle of 19.5° with the bisector axis

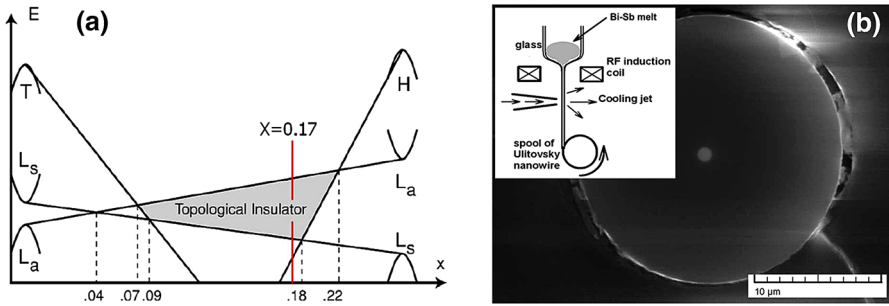


Fig. 1 (a) Schematic representation of band energy evolution of $\text{Bi}_{1-x}\text{Sb}_x$ as function of x . (b) Scanning electron microscope cross sections of the $1.0\text{-}\mu\text{m}$ $\text{Bi}_{0.83}\text{Sb}_{0.17}$ wire in its glass coating. The *inset* illustrates the Ulitovsky method for synthesizing long, small-diameter wires in a glass coating (Color figure online)

C_1 in the bisector-trigonal plane. Because bulk Bi-Sb crystals are difficult to grow successfully, special techniques must be employed to avoid constitutional supercooling and the resulting segregation. With the Ulitovsky technique owing to the high frequency stirring and high speed crystallization ($> 10^5$ K/s) involved it is possible to obtain homogeneous monocrystalline $\text{Bi}_{0.83}\text{Sb}_{0.17}$ nanowires. Encapsulation of the $\text{Bi}_{0.83}\text{Sb}_{0.17}$ filament in glass protects it from oxidation and mechanical stress. A scanning electron microscope image of a cross-section of the $1.0\ \mu\text{m}$ $\text{Bi}_{0.83}\text{Sb}_{0.17}$ wire in its glass coating is shown in Fig. 1b.

The samples for the measurements were cut from long wires, with samples ranging in length from 3 to 0.5 mm. They were then mounted on special foil-clad fiberglass plastic holders. Electrical contact between the nanowire and the copper foil was made with In-Ga eutectic solder. This type of solder consistently makes good contacts compared with other solders with low melting points.

We carried out magnetic field-dependent resistance $R(B)$ measurements in the range of 0–14 T at the International Laboratory of High Magnetic Fields and Low Temperatures (Wroclaw, Poland) and employed a device that tilts the sample axis with respect to the magnetic field and also rotates the sample around its axis. We used the magnetic field modulation technique to measure Shubnikov de Haas (SdH) oscillations. The amplitude of the oscillatory field is 45 Oe. This technique, that is very sensitive, allowed us to register the amplitude of the oscillations directly at the lock-in amplifier output.

3 Results and Discussion

Quantum confinement effects, which influence the alloy band parameters have been predicted for alloy $\text{Bi}_{1-x}\text{Sb}_x$ films [7],[8]. In a $\text{Bi}_{1-x}\text{Sb}_x$ thin film, the L -point band gap depends upon the film thickness t as $\sim t^{-1}$ [9]. Similar quantum confinement effects can be expected in $\text{Bi}_{1-x}\text{Sb}_x$ nanowires [10]. The insert in Fig. 2a shows the temperature dependence of the relative resistance R/R_{300} for Bi nanowires with d values varying from 650 nm down to 45 nm. According to the semimetal-to-semiconductor transformation in Bi nanowires [11], the $R(T)$ dependences exhibit

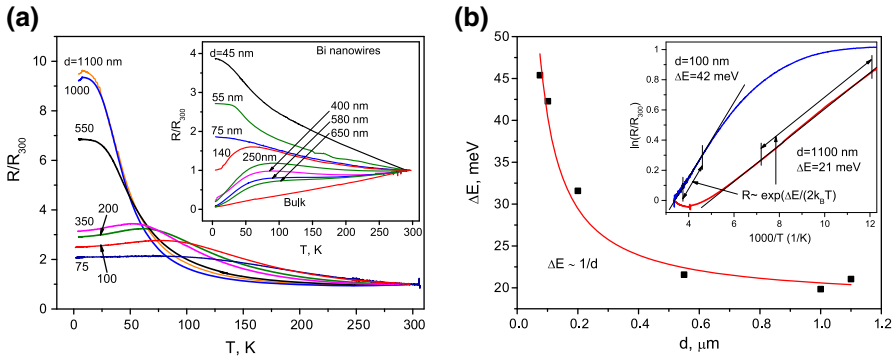


Fig. 2 (a) Temperature dependence of the relative resistance for $\text{Bi}_{0.83}\text{Sb}_{0.17}$ nanowires. *Inset* Temperature dependence of the relative resistance for Bi nanowires. (b) Dependence of the energy gap ΔE on $\text{Bi}_{0.83}\text{Sb}_{0.17}$ nanowires diameter. The data are well approximated by the equation of the energy gap growth with decreasing nanowires diameter $\Delta E \sim 1/d$. *Inset* The Arrhenius plot of R/R_{300} in 1100- and 100-nm $\text{Bi}_{0.83}\text{Sb}_{0.17}$ nanowires indicates a thermal activation behavior with activation gaps of $\Delta E = 21$ and 42 meV, respectively (Color figure online)

”semiconductor” behavior. The temperature dependence values of the relative resistance R/R_{300} for $\text{Bi}_{0.83}\text{Sb}_{0.17}$ nanowires are shown in Fig. 2a. At intermediate temperatures ($T > 100$ K) we observe effects, consistent with quantum confinement effects in our nanowires that would increase the L -point energy gap ΔE and, thus, induce a steeper thermally activated semiconductor behavior in the cases of the small diameter nanowires. However, at low temperatures, the resistance tends to saturate. We interpret the saturation by considering that the conductivity of the topological surface states reduces the overall nanowire resistance. The greater the relative influence of surface states with decreasing nanowire diameter, the stronger the effect of reducing resistance. The Arrhenius plot (see insert in Fig. 2b) of R/R_{300} in 1100- and 100-nm $\text{Bi}_{0.83}\text{Sb}_{0.17}$ nanowires indicates a thermal activation behavior with activation gaps of $\Delta E = 21$ and 45 meV, respectively. The value observed for 1100-nm nanowires is interesting since these are very large diameter nanowires where quantum confinement effects can be expected to be negligible. In this case, considering experimental error, there is agreement between our experimental value and the value of the gap of bulk $\text{Bi}_{0.83}\text{Sb}_{0.17}$. The temperature ranges of exponential growth of resistance $R(T) \sim \exp(\Delta E/2k_B T)$ are also shown. With decreasing nanowire diameter, this temperature range shifts into a higher temperature, which can be explained as follows: First, a rise in the energy gap increases the effective temperature of the smearing of the energy spectrum. Second, the relative influence of the surface states increases with decreasing nanowire diameter, and reduced resistance of the nanowire will be noticeable at higher temperatures. The dependence of the energy gap ΔE on $\text{Bi}_{0.83}\text{Sb}_{0.17}$ nanowire diameter is shown in Fig. 2b; it is well approximated by the equation of energy gap growth with decreasing nanowire diameter $\Delta E \sim 1/d$. This dependence is related to the fact that in $\text{Bi}_{0.83}\text{Sb}_{0.17}$ nanowires there are only carriers in the L -point (see Fig. 1a).

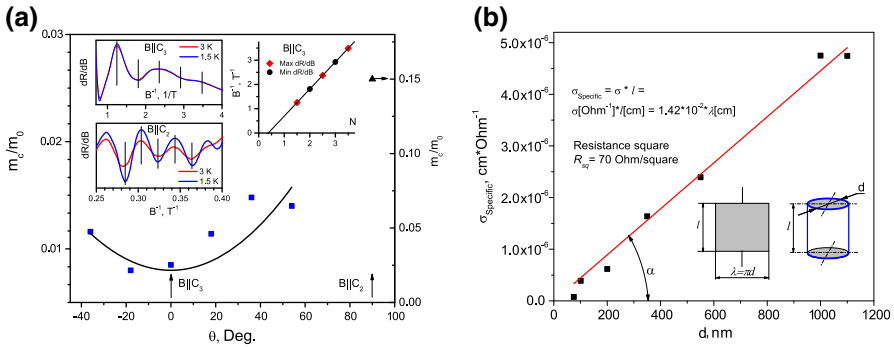


Fig. 3 (a) Angular dependence of cyclotron mass m_c of carriers obtained from SdH oscillations for 200-nm $\text{Bi}_{0.83}\text{Sb}_{0.17}$ nanowire, $B \perp I$. The left two panels of the insets show SdH oscillations in dR/dB measured at 3 and 1.5 K at $B \parallel C_3$ and $B \parallel C_2$ crystallographic axes. The right panel shows Landau-level fan diagrams for SdH oscillations in dR/dB measured at 3 and 1.5 K at $B \parallel C_3$. (b) Dependence of specific conductivity of $\text{Bi}_{0.83}\text{Sb}_{0.17}$ nanowires on nanowire diameter at $T=4.2$ K. The data are well approximated by a straight line; the square resistance R_{sq} of surface states, $R_{sq}=70$ Ohm is calculated from the line slope. Inset Schematic drawing of the transformation of 2D surface states of nanowires into 2D film (Color figure online)

In their research investigating surface states in TI $\text{Bi}_{0.91}\text{Sb}_{0.09}$ (111) through measurements of the weak-field Hall effect and SdH oscillations, Qu et al. [12] discovered that the holelike surface band displays an unexpectedly high mobility ($23,000\text{--}85,000 \text{ cm}^2 \text{ V}^{-1} \text{ s}^{-1}$). We were interested in verifying whether such 2D surface carriers exist in our 200-nm nanowires of $\text{Bi}_{0.83}\text{Sb}_{0.17}$. In our nanowires, the C_3 axis is inclined from the nanowire axis by $\sim 70^\circ$, which warrants carrying out an investigation into transverse magnetoresistance (TMR). We measured TMR when $B \perp I$ for several orientations of the magnetic field near the direction $B \parallel C_3$ and at $B \parallel C_2$. In this case, SdH oscillations at various orientations of the magnetic field were observed. Using experimental data obtained at two different temperatures ($T = 3$ and 1.5 K), we calculated the cyclotron masses for various directions of the transverse magnetic field. Figure 3a shows the angular dependence of cyclotron mass m_c of carriers for 200-nm $\text{Bi}_{0.83}\text{Sb}_{0.17}$ nanowire. For $B \parallel C_3$ and $B \parallel C_2$ directions of magnetic fields, the cyclotron masses and Dingle temperatures equal $8.5 \times 10^{-3} m_0$, 9.4 K, and $1.5 \times 10^{-1} m_0$, 2.8 K, respectively. Landau-level fan diagrams for SdH oscillations in dR/dB measured at 3 and 1.5 K at $B \parallel C_3$ are shown in the insert in Fig. 3a. All the data lie on a straight line that intersects the N axis at 0.4, suggesting the Dirac case spectrum. The slope of the extrapolated straight line gives a frequency F of 0.9 T. The obtained frequency, which is directly related to the cross-section of the Fermi surface A via Onsager relation $F = (\hbar/(2\pi e))A$, gives Fermi wave vector $k_F = 0.0052 \text{ \AA}^{-1}$, which corresponds to the surface carrier density $n_S = k_F^2/4\pi = 2.2 \times 10^{10} \text{ cm}^{-2}$. Knowing the Dingle temperature and the cyclotron mass, we calculated the surface carrier mobility $\mu_S = 26,700 \text{ cm}^2 \text{ V}^{-1} \text{ s}^{-1}$. However, in other surface areas that are nearly perpendicular to the C_3 axis, we obtained significantly higher mobilities ($\mu_{Smax} = 47,000 \text{ cm}^2 \text{ V}^{-1} \text{ s}^{-1}$) comparable with data in Ref. [12]. It should be noted that the 200-nm $\text{Bi}_{0.83}\text{Sb}_{0.17}$ nanowires were optimal for investigation of SdH

oscillations, with decreasing diameter of the nanowires, the SdH oscillation amplitude decreases. However, in thin $\text{Bi}_{0.83}\text{Sb}_{0.17}$ nanowires ($d \leq 100$ nm) at low temperatures ($1.5 \text{ K} \leq T < 5 \text{ K}$), we discovered the Aharonov–Bohm (AB) oscillations [13] of longitudinal magnetoresistance with a period of one flux quantum, Φ_0 ($\Delta B = \Phi_0/S$, where S is the cross-sectional area of the nanowire). A more in-depth study of the experimental results concerning AB oscillations in $\text{Bi}_{0.83}\text{Sb}_{0.17}$ nanowires will be presented in a separate publication.

Because there is an excitation gap in $\text{Bi}_{0.83}\text{Sb}_{0.17}$ nanowires, transport in nanowire samples at low temperatures will be dominated by the surface states. The conductance will be proportional to the circumference of the nanowire rather than the area [5]. The dependence of the specific conductivity σ_{Specific} of $\text{Bi}_{0.83}\text{Sb}_{0.17}$ nanowires on nanowire diameter at $T = 4.2 \text{ K}$ is shown in Fig. 3b, $\sigma_{\text{Specific}} = \sigma \times l$, where σ is the sample conductance and l is the sample length. The data are well approximated by a straight line, which proves that the surface states play a key role in nanowire conductance. The square resistance R_{sq} of the surface states of the nanowires is calculated to be 70 Ohm. The square resistance is inversely proportional to the product $n_S \times \mu_S$, where n_S is the 2D carrier density and μ_S is the 2D carrier mobility. If the 2D carrier concentration $n_S = 2.2 \times 10^{10} \text{ cm}^{-2}$ obtained for the surface area normal to the C_3 axis was the same in all surface areas, we would have huge 2D mobility. However, the surface carrier concentration is much higher in other surface areas.

4 Conclusions

We have investigated the temperature dependence of resistance of TI $\text{Bi}_{0.83}\text{Sb}_{0.17}$ nanowires with varying diameters ($75 \text{ nm} \leq d \leq 1100 \text{ nm}$), obtained by radio frequency casting in a glass capillary. Owing to the quantum size effect, the energy gap ΔE with decreasing diameter of the nanowires (d from 1100 nm down to 75 nm) increases as $\Delta E \sim 1/d$ (for diameter $d = 1.1 \mu\text{m}$ and $d = 75 \text{ nm}$, $\Delta E = 21$ and 45 meV, respectively). Surface states manifest themselves as decreasing resistivity at low temperatures. The SdH oscillations observed in $\text{Bi}_{0.83}\text{Sb}_{0.17}$ nanowires at $T = 1.5 \text{ K}$ demonstrate the existence of high mobility ($\mu_S = 26,700\text{--}47,000 \text{ cm}^2\text{V}^{-1}\text{s}^{-1}$) 2D carriers in the surface areas of the nanowires, which are nearly perpendicular to the C_3 axis. From the linear dependence of nanowire conductance on nanowire diameter at $T = 4.2 \text{ K}$, we calculated the square resistance R_{sq} of the surface states of the nanowires to be only 70 Ohm.

Acknowledgments This work was supported by STCU grant 5986, NSF PREM 1205608, NSF STC 1231319 and the Boeing Co.

References

1. D. Hsieh, D. Qian, L. Wray, Y. Xia, Y.S. Hor, R.J. Cava, M.Z. Hasan, *Nature* **452**, 970 (2008)
2. D. Hsieh, Y. Xia, L. Wray, D. Qian, A. Pal, J.H. Dil, F. Meier, J. Osterwalder, G. Bihlmayer, C.L. Kane, Y.S. Hor, R.J. Cava, M.Z. Hasan, *Science* **323**, 919 (2009)
3. V.S. Edelman, *Adv. Phys.* **25**, 555 (1976)
4. Y. Liu, E. Allen, *Phys. Rev. B* **52**, 1566 (1995)

5. L. Fu, C.L. Kane, Phys. Rev. B **76**, 045302 (2007)
6. D. Gitsu, L. Konopko, A. Nikolaeva, T.E. Huber, Appl. Phys. Lett. **86**, 102105 (2005)
7. S. Tang, M. Dresselhaus, Nano Lett. **12**, 2021 (2012)
8. S. Tang, M. Dresselhaus, Nanoscale **4**, 7786 (2012)
9. S. Tang, M. Dresselhaus, Phys. Rev. B **86**, 075436 (2012)
10. S. Tang, M. Dresselhaus, Phys. Rev. B **89**, 045424 (2014)
11. Y. Lin, X. Sun, M.S. Dresselhaus, Phys. Rev. B **62**, 4610 (2000)
12. D. Qu, S. Roberts, G. Chapline, Phys. Rev. Lett. **111**, 176801 (2013)
13. S. Washburn, R.A. Webb, Adv. Phys. **35**, 375 (1986)